



Available online at www.sciencedirect.com

ScienceDirect

journal homepage: www.intl.elsevierhealth.com/journals/dema



Characterization and toxicity evaluation of air-borne particles released by grinding from two dental resin composites *in vitro*

L.M.A. Camassa^{a,1}, T.K. Ervik^{a,1}, F.D. Zegeye^a, I. Mdala^{b,d}, H. Valen^c, V. Ansteinsdottir^d, S. Zienolddiny^{a,*}

^a National Institute of Occupational Health, Oslo, Norway

^b Institute of Health and Society, University of Oslo, Oslo, Norway

^c Nordic Institute of Dental Materials, Oslo, Norway

^d Oral Health Centres of Expertise in Eastern Norway, Oslo, Norway

ARTICLE INFO

Article history:

Received 1 October 2020

Received in revised form

29 March 2021

Accepted 29 March 2021

Keywords:

Dental composites

Diamond burs

Characterization

Toxicity

ABSTRACT

Objective. The project aims to evaluate whether inhalation of particles released upon grinding of dental composites may pose a health hazard to dentists. The main objective of the study was to characterize the dust from polymer-based dental composites ground with different grain sized burs and investigate particle uptake and the potential cytotoxic effects in human bronchial cells.

Methods. Polymerized blocks of two dental composites, Filtek™ Z250 and Filtek™ Z500 from 3M™ ESPE, were ground with super coarse (black) and fine (red) burs inside a glass chamber.

Ultrafine airborne dust concentration and particle size distribution was measured real-time during grinding with a scanning mobility particle sizer (SMPS). Filter-collected airborne particles were characterized with dynamic light scattering (DLS) and scanning electron microscopy (SEM).

Human bronchial epithelial cells (HBEC-3KT) were exposed to the dusts in dose-effect experiments. Toxicity was measured with lactate dehydrogenase (LDH) assay and cell counting kit-8 (CCK8). Cellular uptake was observed with transmission electron microscopy (TEM). **Results.** Airborne ultrafine particles showed that most particles were in the size range 15–35 nm (SMPS). SEM analysis proved that more than 80% of the particles have a minimum Feret diameter less than 1 μm. In solution (DLS), the particles have larger diameters and tend to agglomerate. Cell toxicity (LDH, CCK8) is shown after 48 h and 72 h exposure times and at the highest doses. TEM showed presence of the particles within the cell cytoplasm.

Significance. Prolonged and frequent exposure through inhalation may have negative health implications for dentists.

© 2021 Published by Elsevier Inc. on behalf of The Academy of Dental Materials.

* Corresponding author at: Head and Lead Research Professor, Section for Occupational Toxicology, National Institute of Occupational Health, Oslo, Norway.

E-mail address: shan.zienolddiny@stami.no (S. Zienolddiny).

¹ Equal contribution.

<https://doi.org/10.1016/j.dental.2021.03.011>

0109-5641/© 2021 Published by Elsevier Inc. on behalf of The Academy of Dental Materials.

1. Introduction

Polymer based dental composites are now the most widely used material in restorative dentistry. They consist of inorganic filler particles, organic polymer matrix made of different methacrylate resins and a coupling agent binding the inorganic filler to the polymer matrix [1]. In the drive to develop superior dental composite materials, the unique properties of nanomaterials is certainly attractive. Dental composite materials contain a mixture of micro- and nanosized particles [2]. Nanoparticles are added mainly to increase filler load and thereby increase mechanical strength, diminish wear and reduce polymerization shrinkage of the composite [3]. Nanoparticles can also provide desired aesthetic properties to the material [4–6]. Hence, the use of nanoparticles in these materials have increased in the last decade. In addition to high levels of nanosized silica fillers, dental composites contain mixtures of other elements that increase radiopacity such as barium and aluminium [3,7].

As the use of dental composites in dentistry is increasing, there is a concern that dentists and other dental health workers may be exposed to nanoparticles released from materials, as well as nanoparticles generated during removal of fillings with burs and during polishing. The health risks associated with such exposure in the dental setting is not fully elucidated.

Studies have reported that particles of various sizes, including nanoparticles, are generated in high number concentrations, $>10^6$ cm³, during procedures such as high speed grinding of dental composites [8,9]. Whether nanofillers are released upon the grinding of dental composites is, however, still unclear [10].

Van Landuyt et al. [8,9] identified the release of single nanofiller particles, while Bogdan et al. [11] mostly observed organic nanoparticles originating from thermal decomposition of the resin matrix. In a study by Bradna Pavel et al., the bur coarseness and the bur speed was varied. No increase in particle concentration above background levels were observed when a fine diamond bur was used at 15 000 rpm compared to coarser burs used at higher speed (100 000 rpm) [12].

Knowledge regarding indoor air quality in dental clinics from a chemical perspective are still scares. It has been shown that dental drilling procedures may cause an increase in particle concentrations in the dental office, and that the concentration was highest for particles under 0.5 μ m [13]. A study from Helmis et al. performed in several university clinics found that on most days, the daily concentration values of particulate matter <10 μ m (PM10) exceeded the limit of 50 μ g m⁻³ described by the Directive 1999/30/EC [14–17]. Factors that influence the particle concentrations during different clinical procedures are the use of water spray and ventilation in the room [18].

Dental health workers can potentially be exposed to hazardous dust or particles [19] and methacrylate resin vapour [20,21] where inhalation and skin exposure to some of these materials might increase the risk of work-related illness and occupational diseases [22–24]. An extensive literature review on occupational health problems in modern dentistry from Australia, suggests that a variety of health hazards as percutaneous exposure incidents (PEI), exposure to infectious agents,

including bioaerosol, respiratory hypersensitivity, are found in dental practises [25].

The characteristics of particles including size and chemical composition may affect their toxicity. It is known that the smallest particles (i.e. nanoparticles) are accumulated in deeper parts of the respiratory system. Depending on particle size, most of the nanoparticles (<100 nm) are found in the alveolar region of the lungs [26]. Once in the alveolar region they may cause local pulmonary inflammatory reactions or translocate into circulation [27–29]. An *in vitro* study from Ansteinsson et al., showed that commonly used inorganic filler particles in dental composites released during dental restoration, could potentially trigger and maintain inflammatory reactions mediated by pro-inflammatory interleukin IL-6 and chemoattractant IL-8 [29].

The main objective of this study was to perform an in-depth characterization of the dust with regards to size distribution and morphology of particles generated from two polymerized composites upon grinding with burs with different grain sizes, and while keeping the speed of the bur constant. The collected particles was used further to investigate the particle uptake and the potential cytotoxic effects on human bronchial cells.

2. Materials and methods

2.1. Dental composites

Two commercially available and commonly used dental composites were used in this study and are described by the manufacturer as follows: Filtek™ Z250 and Filtek Z500™ by 3 M™ ESPE™. The Filtek™ Z250 is a microhybrid containing zirconia/silica fillers (0.01–3.5 μ m diameter) loaded to 60 vol.%. Filtek™ Z250 restorative contains BIS-GMA, UDMA, and BIS-EMA resins. Filtek™ Z500 is a nanohybrid containing a combination of aggregated 5–20 nm zirconia/silica fillers (so-called *nanoclusters* with average diameter 0.6–1.4 μ m) and non-aggregated 20 nm silica filler (Fig. 1). The inorganic filler loading is about 78.5% by wt (59.5% by volume). Filtek™ Z500 restorative contains bis-GMA, UDMA, TEGDMA, and bis-EMA resins. More information on the dental material can be found in the technical profile of 3 M™ ESPE™ Filtek™ Z250 and Z500™ Universal Restorative materials (3 M ESPE Filtek™ Z250 and Z500 Universal restorative).

2.2. Dental composites dust preparation and collection

For each composite, specimens of 2 mm \times 2 mm \times 25 mm were prepared in molds of stainless steel and light cured for three times 20 s on two side using Bluephase 20i (Ivoclar Vivadent) with and irradiance claimed by the manufacturer of 1200 mW/cm². The weight of each block was approximately 0.2 g and the blocks were weighed before and after grinding to determine the amount of material ground. The blocks were ground inside of a chamber with hands aperture with black (super coarse, grain size 181 μ m) and red (fine grain size 40 μ m) diamond burs (40 000 rounds per minute) to create four different dental dust samples: Filtek™ Z250 red and black, and Z500™ red and black, respectively. The dental dust was collected using a GSP conical inhalation sampler (GSA

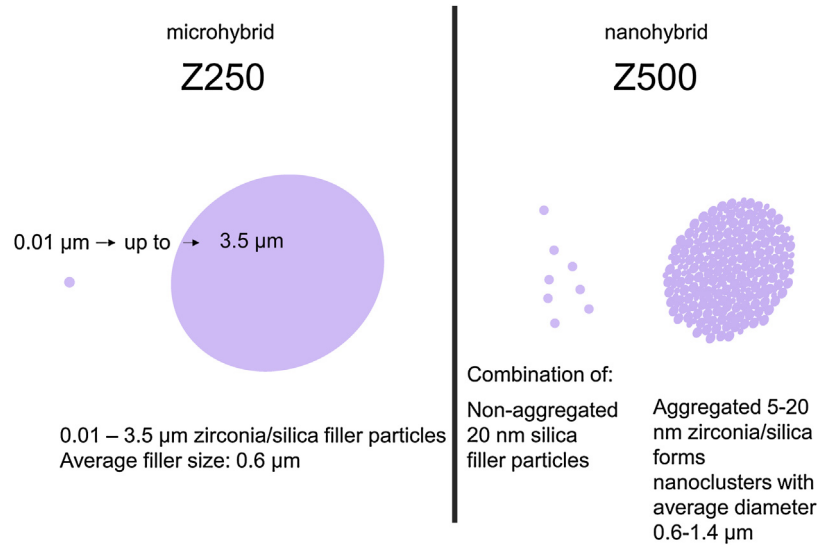


Fig. 1 – Schematic illustration of the two dental composites considered in the study.

Messgerätebau GmbH, Ratingen, Germany) with a cone diameter of 10 mm connected to a sampling pump with air flow approximately of 10 l/min. The GSP sampler contained a cassette with a filter with pore size of 5 μm (Millipore). Approximately the same amount of composite was ground for each block. The collected dental particles came from three different sampling campaigns and were, eventually, mixed to one pooled sample which was further used in the toxicity experiments.

2.3. Scanning electron microscopy (SEM)

The size distribution of all three batches as well as the pooled sample was investigated by SEM-EDX. The sample procedure for the dry collected sample was as follows: a small part of collected sample was drawn through a nozzle and impacted on a polycarbonate (PC) filter with pore size 0.2 μm in an anti-static sampler. The filter was precoated with approximately 10 nm platinum (Pt) in a Cressington 208 h sputter coater (Cressington Scientific Instruments Ltd., Watford, United Kingdom). Approximately 1 cm^2 piece of the filter was cut out, fixed on a 10 mm aluminium stub covered with double-sided carbon adhesive. Spots of carbon cement (Leit-C) were added to the sides of the stub to assure a good conductivity between filter and stub. In addition, the pooled sample was suspended in dispersion medium and sonicated (same as for DLS procedure). For the suspended particles, the dental composite particles were filtered through a PC filter with pore size 15 nm. A piece of approximately 8 × 8 mm piece of the filter was cut out, fixed on a 10 mm aluminium stub covered with double-sided carbon adhesive discs and spots of carbon cement (Leit-C, Agar Scientific Ltd.) were added to the sides of the stub to assure a good conductivity between filter and stub. The samples were coated with a 10 nm Pt layer. The specimens were analysed with a field emission scanning electron microscope SU6600 FESEM (Hitachi, Tokyo, Japan) operated with an acceleration voltage of 15 keV, analytical working distance of 10 mm, electron probe current 7–8 nA and backscatter imaging (BEI) mode

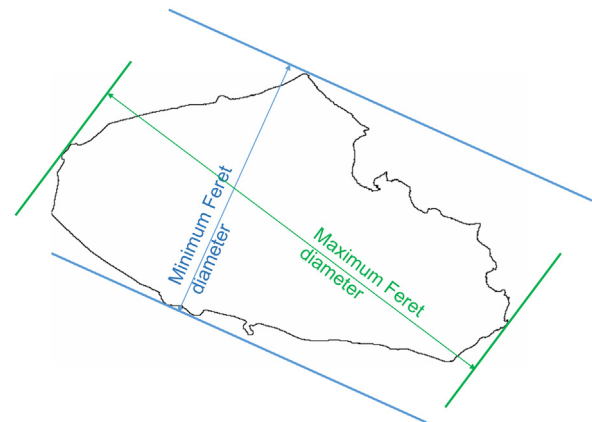


Fig. 2 – Sketch showing the minimum and maximum Feret diameters.

using a solid-state detector. Automated analysis on the shape and size of particles was performed using the feature module of the esprit software (Bruker-AXS Microanalysis GmbH, Berlin, Germany). As a first step in the automatic particle analysis, high contrast (BE) images were acquired from the SEM at a magnification of 2000× at a resolution of 1800 × 1350 pixels (pixel size = 0.03 μm). The size of at least 2000 particles from each sample was obtained from the automatic analysis. The minimum Feret distance is equal to the smallest distance between two parallel tangents to the particle border and was chosen to represent the particle size (Fig. 2).

2.4. Dust dispersion protocol and measurement by dynamic light scattering (DLS)

The pooled dental dust sample was used for the cell exposures after sonication. Filtek™ Z250 red and black and Filtek™ Z500 red and black were suspended in a dispersion medium (0.05% BSA and MilliQ water) to a final concentration of 2.56 mg/ml. Dispersion methodology and stock concentration were

chosen in accordance with the Nanogenotox protocols [30]. The solution with particles was sonicated using a 400 W Branson Sonifier S-450D (Branson Ultrasonics Corp., Danbury, CT, USA) equipped with a standard 13 mm disruptor horn (Model number: 101-147-037). Sonication was run for 15 min at 400 W and 10% amplitude. After sonication all samples were analysed with DLS and the hydrodynamic diameter measurements were conducted in dispersion medium. The measurements were done by a ZetaSizer (ZetaSizer Nano ZS, Malvern Instruments Ltd., Malvern, UK) using refractive index for a composite of 1.59. The analysis was conducted on three independent dispersed batches of pooled dental dust samples. Z-Average (Z-Ave) and polydispersity index (PDI) was measured. Z-Average gives the mean value of the hydrodynamic diameter of the particle and PDI measures the width of the particle size distribution.

2.5. Scanning mobility particle sizer (SMPS) measurements

Particle number concentrations were measured inside of the chamber during grinding using an SMPS (model 3938, TSI Inc., Shoreview, MN, USA). The SMPS consisted of the following TSI components: 3082 Electrostatic Classifier, 3756 Ultrafine Condensation Particle Counter (CPC, a long differential mobility analyzer (3081 DMA) and a 0.0457 cm diameter orifice aerosol inlet impactor. With the SMPS-parameters used in this study, particles in the range of 9–160 nm electrical mobility diameter were measured during grinding. A scan time of 30 s was used and was started simultaneously with the grinding. An anti-static tube of length 20 cm was connected to the impactor inlet of the Electrostatic Classifier and fixed inside the chamber. The tube creates a delay in the measurements and two scans passed before higher concentrations of nanoparticles were measured. Background levels were reached before starting a new grinding procedure. Two measurements were performed for each material and bur.

2.6. Exposure of human bronchial epithelial cells (HBEC-3KT), cell culture conditions and exposure doses

Human bronchial epithelial cell line HBEC-3KT, immortalised with CDK4 and hTERT, were used in all experiments. HBEC-3KT were maintained under standard growth conditions of 5 % of CO₂ and 37 °C [31,32]. Cell medium was a 1:1 mixture of LCH-9 (Gibco) and RPMI (Fisher) medium. Plates were pre-coated with 0.01 % collagen (Type I, PureCol® from Advanced BioMatrix). For each assay, one day prior to the experiment, HBEC-3KT cells were seeded at different densities depending on the length of exposure time and the growth area of the plate used: 2.5×10^4 cells/cm² for 24 h, 1.25×10^4 cells/cm² for 48 h and at 8.3×10^3 cells/cm² for 72 h. The exposure took place the following day. At the end of each exposure, the confluency of the cells was comparable. HBEC-3KT cells were exposed to Filtek™ Z250 (red and black) and Filtek™ Z500 (red and black) in the following concentrations; 0, 5, 10, 20, 40 and 80 µg/cm². The time of exposure was 24 h, 48 h and 72 h. Doses and time points were chosen because of their relevance for occupational exposure situations. Number of biological repli-

cates for each condition inside of the experiment is three and each experiment is repeated three times.

2.7. Cellular toxicity of filler materials

After each time of exposure, HBEC-3KT cells were tested for cell viability and cell toxicity using a cell counting kit-8 (CCK8) (Sigma-Aldrich) and lactate dehydrogenase (LDH) cytotoxicity assay (LDH-kit) (CyQUANT™, ThermoFisher). CCK-8 and LDH assays are colorimetric tests based on two different metabolic reactions. They are measuring the amount of activity of living cells dehydrogenase (CCK8) and the activity of LDH dehydrogenase typical of damaged cells. The colorimetric assays are based on the conversion of the tetrazolium salt (INT) dye into a red formazan by electrons reduction, which can be quantified spectrophotometrically. The two assays combined give us more information on cell integrity and toxicity. Additionally, the convenience is that it is possible to use the same sample for both of the assays.

CCK8 absorbance was measured at 450 nm and this value is directly proportional to the number of living cells. LDH absorbance was measured at 490 nm and released values in percentage were obtained using the following formula:

$$\begin{aligned} & \%LDH \text{ released (cytotoxicity)} \\ &= \frac{\text{Compound-treated LDH activity} - \text{Spontaneous LDH activity}}{\text{Maximum LDH activity} - \text{Spontaneous LDH activity}} \\ & \times 100 \end{aligned}$$

The background signal was measured at 680 nm and subtracted from the 490 nm absorbance value. The absorbance were measured using a Spectramax-i3 and a Soft Max®Pro microplate data acquisition and analysis software (Molecular Devices).

2.8. Cellular uptake experiments with transmission electron microscopy

HBEC-3KT cells were exposed to the particles for 24 h and 72 h. At day one, the cells are exposed to Filtek™ Z500 black dental composites at the concentration of: 5 µg/cm² and 40 µg/cm². After the exposure, the cells were fixed with a solution of 2,5% Glutaraldehyde (Fluka) in phosphate buffer saline (PBS) solution. The cells were washed three times in PBS and post-fixed for 20 min with a solution of 1% OsO₄ (Fluka). The cells were then gently scraped and centrifuged for 5 min at the 13 000 rpm. The temperature was kept constant to not disturb the cells morphology. Porcine skin A gelatine (Electron Microscope Science™) was prepared and cool down at 37 °C and add to the cell pellet to create gelatine blocks. The gelatine blocks were embedded in durcupan mix (ACM-Fluka) and processed for the electron microscopy analysis.

Ultraphin sections were cut at 70–80 nm using a Leica Reichert Ultracut Ultratome and Diatome knife. Sections were contrasted with 2% uranyl acetate for 4 min and rinsed in MillQ water, contrast in lead citrate was avoid to not create deposition and interference during the observation. Sections were examined with a Tecnai-12 transmission electron microscope at 60 kV.

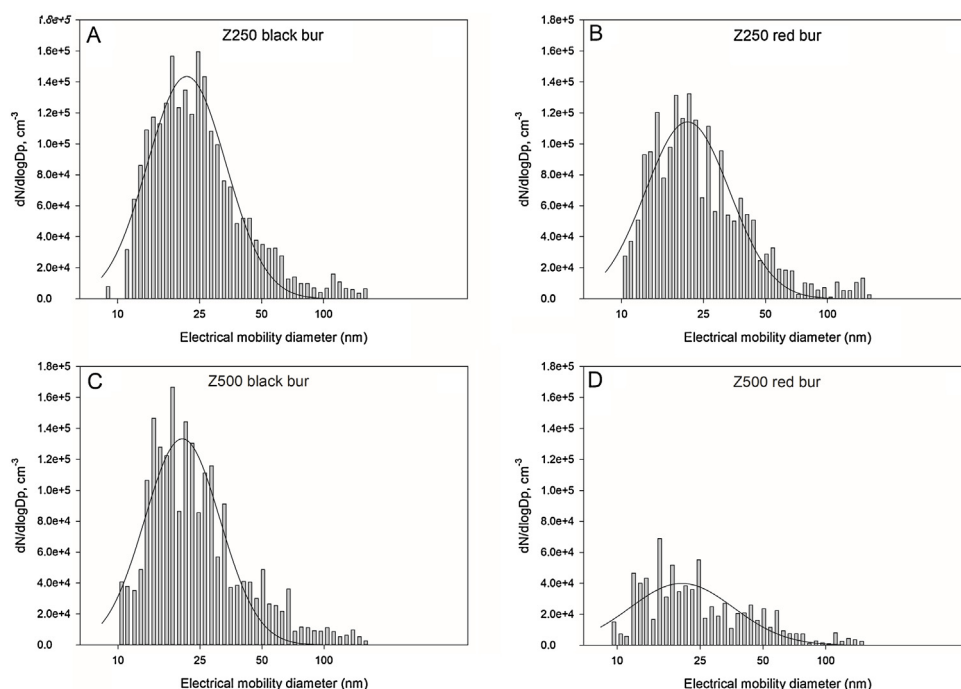


Fig. 3 – Particle number size distribution measured during grinding for **A. Z250 black bur**; **B. Z250 red bur**; **C. Z500 black bur**; **D. Z500 red bur**. Bars represent measured data and line represent the calculated lognormal fit.

2.9. Statistical methods

SEM analysis is Kernel density non parametric distribution of minimum Feret diameter. DLS and CCK8 analysis are multiple comparisons.

To understand the changes in LDH released at different doses and to measure the amount of variability in LDH released between wells, we fitted linear mixed effects models with random effects at the well level. In particular, we considered two-way interaction terms involving time (24 h, 48 h and 72 h) and dose amounts. This helped in explaining the changes in LDH release within each dose amount from one time point to the other. Furthermore, we were able to present and explain the differences in LDH released between dose amounts at each time point using the time–dose interaction term. We also used margin plots to aid in understanding and interpreting of the interaction terms. However, the analyses showed no significant variability in LDH released between wells. All analyses were performed in StataSE 16 and the significance level was set at $\alpha = 0.05$.

3. Results

3.1. Size distribution of particles generated during grinding measured with SMPS

The size distribution and number concentration of particles in the range 9–160 nm, measured inside the chamber during grinding of the different composite materials with burs with different grain size, showed air values in the range of 0.5×10^5 – 1.5×10^5 cm^{-3} (Fig. 3A–D). The majority of measured

particles were in the size range 15–30 nm and no significant differences between the materials were observed. As the grinding is made manually, curves are expected to fluctuate. However, the curves are still observed to have a lognormal distribution (Fig. 3).

3.2. Size distribution of collected particles - SEM

SEM was used to measure the size distribution and to characterize the morphology of generated particles with diameters from 50 nm and up to 8 μm . Kernel density plot of the minimum Feret diameter for the different pooled dental composites dust collected, showed no significant differences in particle size distributions for the four dental dust materials (Fig. 4A). The size distributions between the three individual collected dust samples and the pooled samples were also compared (Supplementary Fig. 1A–D). A high fraction (>80%) of the collected particles were in the sub-micron range and most particles have a minimum Feret diameter of 0.2 μm . This applied to all the individual collected dust samples as well as the pooled samples. Mean minimum Feret diameters for dry particles were in the range 0.44–0.54 μm (Fig. 5). For the particles in solution (denoted wet), a minimum Feret diameter of 0.2 μm was also observed for most particles (Fig. 4B). However, larger variations compared to the dry particles was observed, with mean Feret diameters in the range 0.38–0.59 μm (Fig. 5).

In SEM, both larger inorganic filler particles in Z250 and nanoclusters in Z500 were often observed (Supplementary Fig. 2A and B). Often remnants of the polymerized organic matrix surrounded the particles (Fig. 6A). SEM images of a single filler particle from Z250 and a single nanocluster from Z500, both

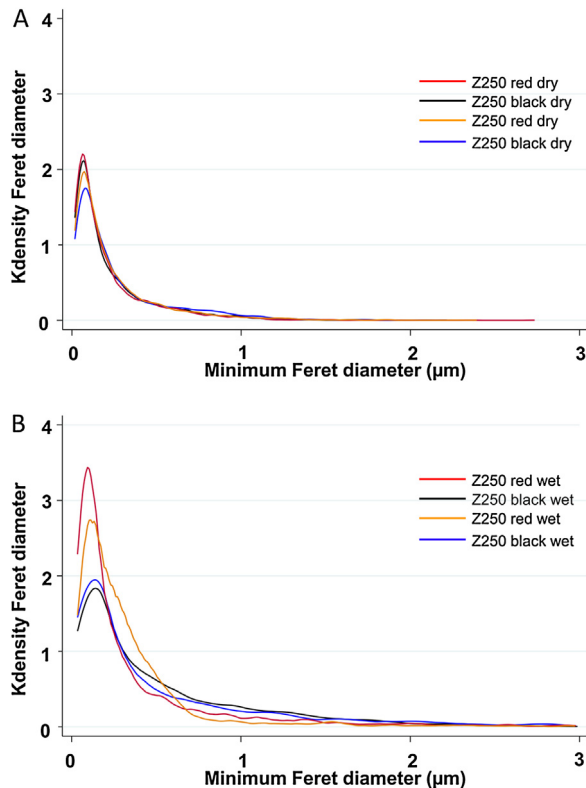


Fig. 4 – Kernel density plot of minimum Feret diameter for the pooled/mixed materials for A. the dry material (as collected at the time of grinding) and B. wet material (sonicated after dissolution in dispersion medium).

Table 1 – Hydrodynamic diameters (Z-Ave) and polydispersity indices (PdI) of the composites.

Filtek™ dental composites	Z-Ave (nm) (SE)	PdI (SE)
Z250 Red	976.00 (113.15)	0.41 (0.05)
Z250 Black	1130.77 (167.49)	0.59 (0.04)
Z500 Red	1318.00 (107.33)	0.47 (0.01)
Z500 Black	1357.80 (201.20)	0.51 (0.05)

ground with black bur, show that the nanoclusters and the filler particles appeared spherical (Fig. 6B, D). However, when magnified images are investigated it is possible to see the individual nanoparticles in the Z500 composites, whereas the surface of a filler particle in Z250 appeared smooth also at high magnification. Similar images were observed for materials ground with the red bur (pictures not shown).

3.3. Hydrophobic size of particles — DLS

The hydrodynamic size distribution of the particles (Fig. 7), shows that amorphous particles from Z250 (red and black) and Z500 red in dispersion medium have mainly three peaks of various nm-size range: peak 1 (201–250 nm), peak 2 (1001–2500 nm) and peak 3 (4000 nm). Z500 black do not show the peak at (201–250 nm), but a peak at (251–1000 nm). The values of Z-average (Z-Ave), polydispersity indexes (PdI) and standard error (SE) are shown in Table 1. DLS analysis of dental particles in dispersion medium showed increased hydrodynamic

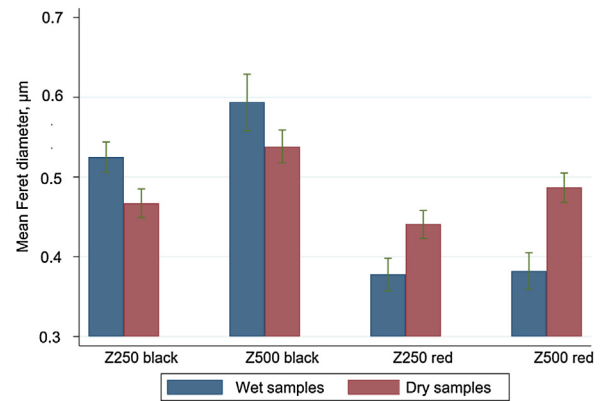


Fig. 5 – Mean Feret diameter for the pooled/mixed samples. Blue bars show the particles filtered from solution and red the dry particles.

diameters and high polydispersity indices indicating that the particles tend to aggregate and agglomerate.

3.4. Cell toxicity and cell viability

Shown in Fig. 8 the cell toxicity response after exposure with Z250 and Z500 ground with red bur (A, C) and black bur (B, D).

After 24 h of exposure with Z250 red bur and black bur (Fig. 8A, B), no cell toxicity is observed at low doses compared to the unexposed group (control). A significant toxicity is observed at the maximal doses. At 48 h and 72 h exposure time, cell toxicity is observed at the concentration of 20 $\mu\text{g}/\text{cm}^2$, 40 $\mu\text{g}/\text{cm}^2$ and 80 $\mu\text{g}/\text{cm}^2$ (Fig. 8A, B; Supplementary Table 1).

Similar dose-effect responses were observed for Z500 ground with red and black bur (Fig. 8C, D; Supplementary Table 1). After 24 h of exposure with Z500 red bur (Fig. 8C), no cell toxicity is observed by low or high doses compared to the control. After 48 h and 72 h, cell toxicity is observed at the doses of 40 $\mu\text{g}/\text{cm}^2$ and 80 $\mu\text{g}/\text{cm}^2$ (Supplementary Table 1). At these exposure times and low doses (5, 10, 20 $\mu\text{g}/\text{cm}^2$), we observed that % LDH released is negative compared to the control. This effect shows that spontaneous LDH released values of not exposed cells are slightly higher than the LDH released values of cells exposed to low doses. Cells exposed with Z500 ground with black bur (Fig. 8D) showed significant ($p < 0.01$) effect of toxicity compared to the control at all concentrations after 24 h. However, this effect is not measurable for 5 $\mu\text{g}/\text{cm}^2$ at the 48 h and 72 h. A significant toxicity ($p < 0.01$) is observed at the doses of 20 $\mu\text{g}/\text{cm}^2$, 40 $\mu\text{g}/\text{cm}^2$ and 80 $\mu\text{g}/\text{cm}^2$.

After 24 h and 72 h, the HBEC-3KT cells were also tested for viability using the CCK-8 assay (Fig. 9). Low doses of Z250 and Z500 (both red bur and black bur) did not show a significant effect on the cell viability when compared to the control (Fig. 9A–D). After 72 h, cell viability is affected at the high doses for all the dental composites. In referral to the control, black particles (Fig. 9B and D) are affecting the cell viability already at 20 $\mu\text{g}/\text{cm}^2$.

At each times of exposure, control cells and cells treated with 80 $\mu\text{g}/\text{cm}^2$ of particles, were observed under a microscope and pictures were taken. No considerable changes in cell morphology were detected (data not shown).

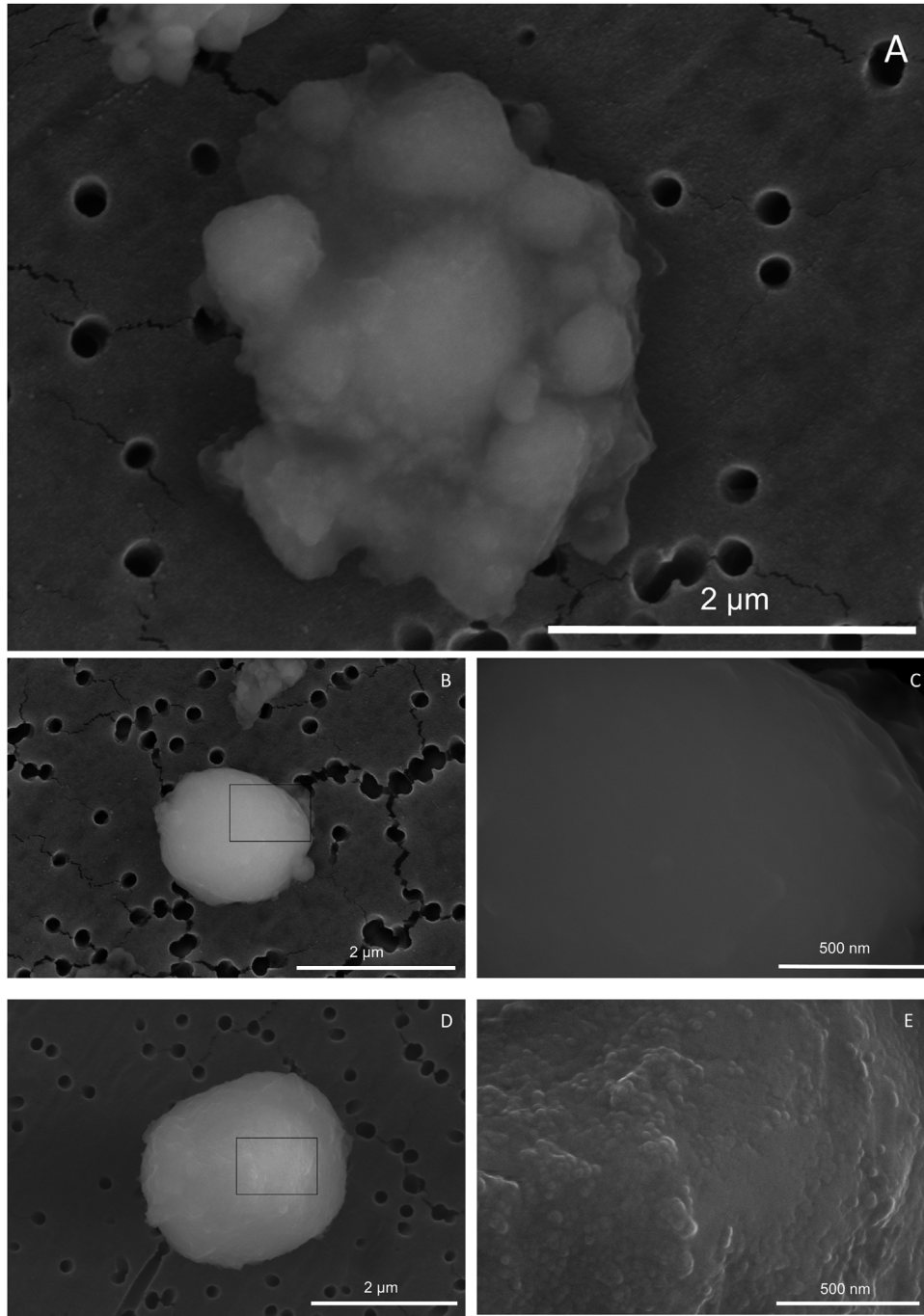


Fig. 6 – A. SEM image of a mixed particle, containing resin and filler particles of various size for Z250 ground with the black bur. **B.** Magnified SEM-image of a spherical shaped filler particle (Z250). **C.** Magnified image of the surface (Z250). **D.** Magnified SEM-image of a spherical shaped nanocluster (Z500). **E.** Magnified image of the surface (Z500). Similar particles were found when these materials were ground with red bur (data not shown).

3.5. Uptake of particles by HBEC-3KT cells

To investigate uptake and intracellular localization of particles, HBEC-3KT cells were exposed to particles (Z500 black) at a concentration of $5 \mu\text{g}/\text{cm}^2$ and $40 \mu\text{g}/\text{cm}^2$ for 24 h and 72 h. Enlarged membrane structured like-vacuoles surrounding the particles were identified after 24 h for both concentrations

of particles. In the unexposed group (control), no particles were observed in smaller vacuoles (Fig. 10A, B). After 72 h exposure, particles were identified in smaller vacuoles compared to 24 h exposure for both concentrations (Fig. 10D, F). No particles were observed inside the nuclei in any of the samples.

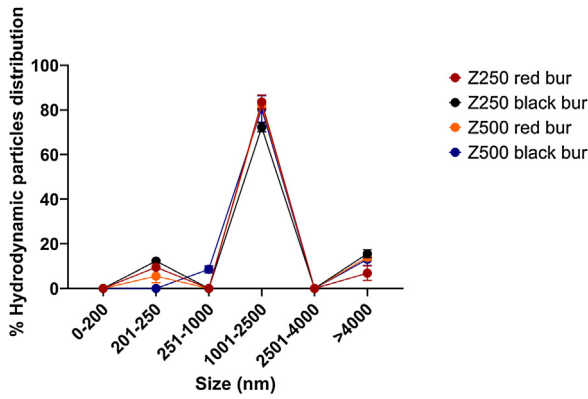


Fig. 7 – % Hydrodynamic particles distribution. The dots in the graph are representing the mean of three independent measurements. Error bars represent standard error (+– SE).

4. Discussion

Previous investigations have showed size distribution curves at the end of grinding when the aerosol stabilizes [8,12]. However, nanoparticles agglomerate with time and the particle size distribution might therefore shift towards larger particle sizes. The majority of particles had diameters in the size range of 15–30 nm for both composite materials which are in the range of the silica nanofillers reported by the manufacturer to exist as individual 20 nm nanoparticles in Filtek™ Z500. Filtek™ Z250 is a microhybrid and consists of nano- and micrometer sized fillers and is therefore expected to have a broader size distribution if filler particles were the origin of nanoparticles. However, the size distribution curves have similar shapes and identical median diameters (20–25 nm) for the four SMPS experiments (Fig. 3). This might indicate that the ultrafine particles detected are not released nanofillers. Bogdan et al. observed no differences in abrasion of samples with and without filler particles and argued that the nanoparticles measured are a condensation aerosol with particles created from the evaporation of resin matrix rather than released

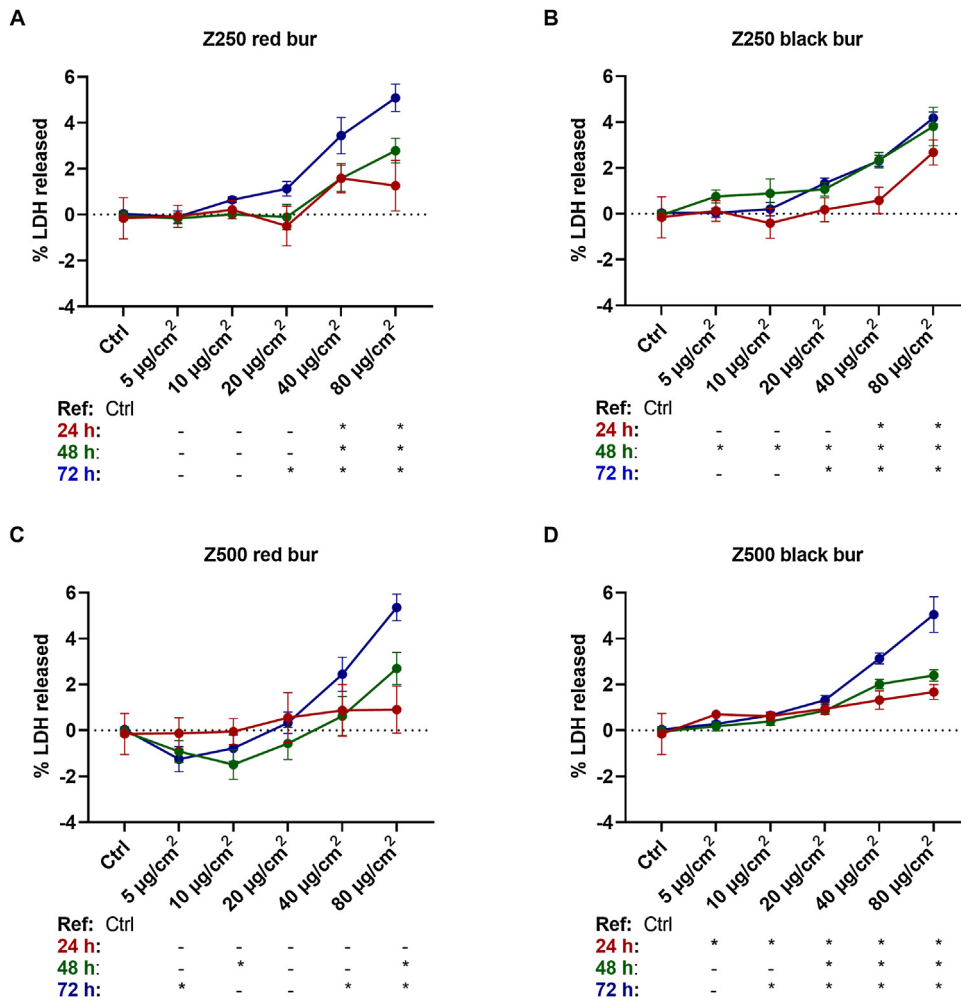


Fig. 8 – % LDH released from HBEC-3KT cells after exposure to four different dental composites. A. Z250 red bur and B. Z250 black bur. C. Z500 red bur and D. Z500 black bur (left). HBEC-3KT cells were exposed to five different doses (5, 10, 20, 40 and 80 µg/cm²) of each dental composites for 24 h 48 h and 72 h. Dots represent the mean of % LDH released, error bars indicates +– β (95% CI). *Significant values compared to the control (p-value = p < 0.05).

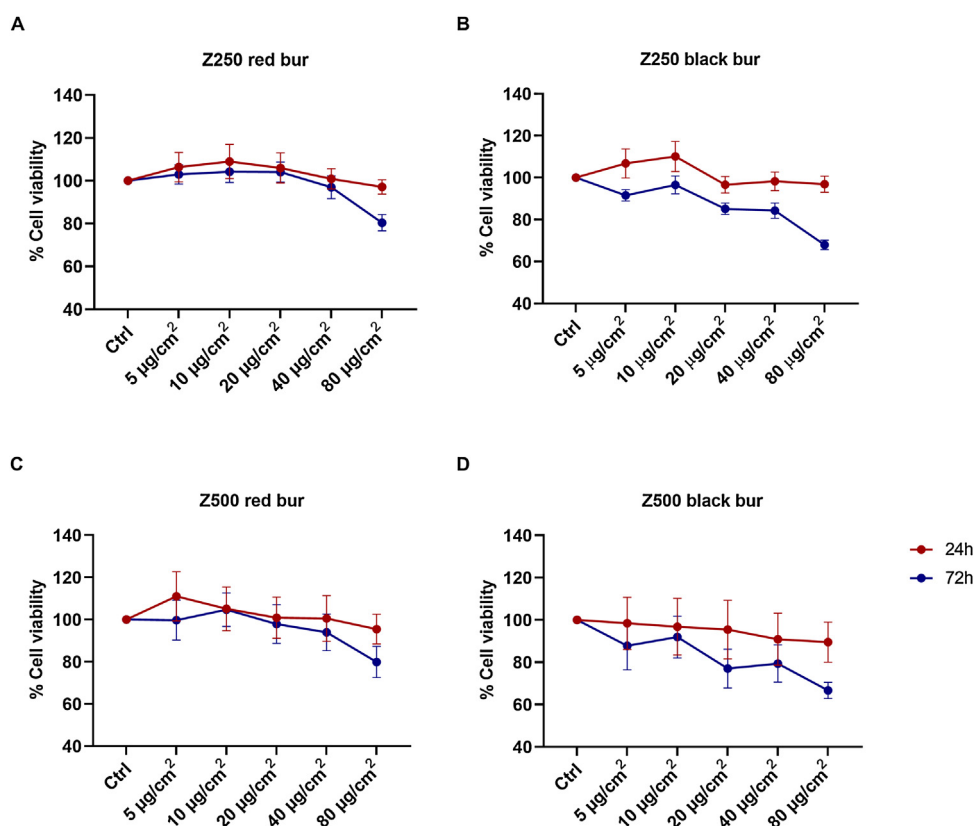


Fig. 9 – % Cell viability after exposure to four different dental composites. HBECK-3KT were exposed for 24 h and 72 h to **A. Z250 red bur** and **B. Z250 black bur** and **C. Z500 red bur** and **D. Z500 black bur**. Dots represent the mean of absorbance at the dose in percentage normalized to the control, error bars indicates \pm SE.

nanofillers [11]. In addition, lubricant from the dental drill generated an oil aerosol in the nanosize range, which also affected their measurements. No individual nanofiller particles with sizes \sim 20 nm were observed in TEM in their study. The same remark on thermal decomposition of the matrix was made by Bradna Pavel et al., which found that the nanoparticle release was not depending on the filler particles size and content [12]. The nanoparticle release was instead depending on the diamond grain size and bur speed. In the present study, both coarse and fine diamond bur running at the same speed generated approximately the same concentration of ultrafine particles (Fig. 3) indicating that the speed might be more important.

Larger filler particles in Z250 and the so-called nanocluster/nanostructures in Z500 were easily recognized when the ground materials were investigated in SEM. Both the nanoclusters and the filler particles appeared spheroidal with smooth surfaces. With higher magnification, the surface of Z500 was seen to be irregular with small (\sim 20 nm) particles visible (Fig. 6E). With the use of SEM no single nanofiller particles were detected. Nevertheless, the existence of such particles cannot be excluded and a further TEM study could better identify the presence of nanofiller particles.

The particle size distribution measured by SEM for the Z500 corresponds well to the size distribution that was measured with ImageJ from high-resolution photomicrographs in TEM on FiltekTM supreme upon grinding by Van Landuyt et al. [9].

The high fraction of sub-micron particles ($>$ 80%) indicates that there is a high fraction of respirable particles that can penetrate down to the alveoli region of the lung. The red bur has a finer grit-size than the black bur and could therefore decrease the particle size released during grinding. A decrease in mean diameter is seen for the red bur compared to the black bur (Fig. 5), however this significance was not observed for Z250 dry samples.

One would also expect the particles in solution to have an increased mean size due to agglomeration, however this was not the case for Z250 red and Z500 red (Fig. 5), and the exact reason for this is not known. For the Z250 black and Z500 black, the mean particle diameter of the wet samples is larger. The filter might influence these analyses, as these are different for the dry and the wet particles. The pores (50 nm) are not visible in the filter substrate used for the particles in solution and it is therefore easier to adjust the contrast for the automatic analysis. A higher number of the smallest particles might therefore be visible.

There are other limitations of the SEM automatic analysis. There are pores with size 0.2 μ m on the filter collecting the dry particles. The contrast was adjusted so that these are not visible in the BE-image. However, the contrast adjustment might cause small particles to disappear. At the magnification of 2000x, the pixel size is on the order of 0.03 to 0.05 μ m depending on the resolution of the image. The mixed particles might cause problems for the automatic analysis since

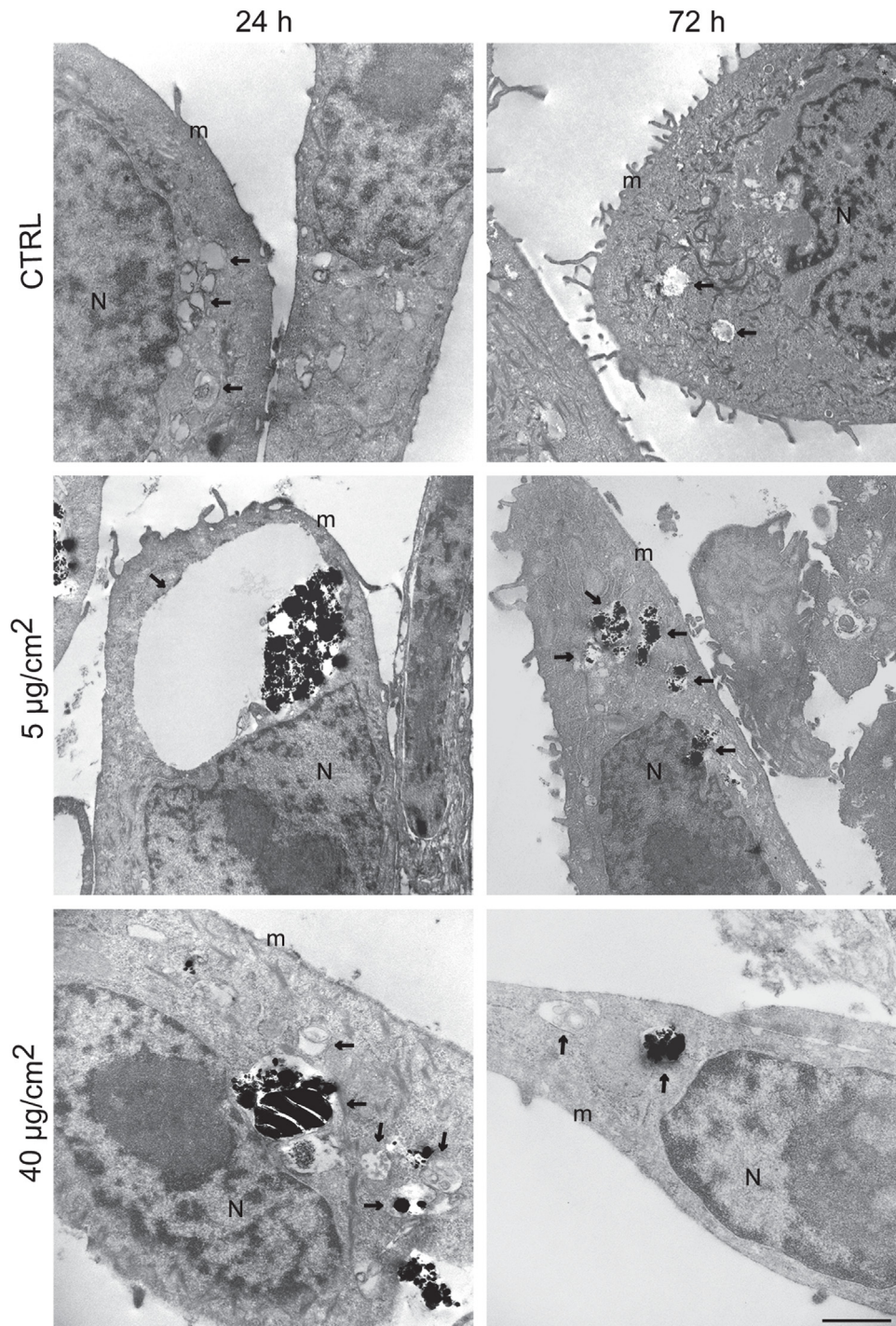


Fig. 10 – Electron micrographs of HBEC-3KT cells engulfing Z500 Black bur. Electron micrographs of HBEC-3KT after 24 h (A, C, E) and 72 h (B, D, F) exposure to $5 \mu\text{g}/\text{cm}^2$ (C, D) and $40 \mu\text{g}/\text{cm}^2$ (E, F) of Z500 black show enlarged membrane invagination (arrows) engulfing the dental composites. In the control, no particles are found. N, nuclei; m, cellular membrane; arrows, vacuoles Scale bar: $2 \mu\text{m}$.

the resin matrix and the filler particles contain elements with significant deviation in atomic number. The topography of relatively large mixed particles can probably also contribute to errors since topography variations also affect brightness. The consequence from the issues listed up above might be that individual nanoparticles below the pixel size are not mea-

sured. Additionally, there might be an underestimation of large particles due to brightness variations.

Dynamic light scattering was used to determine the size and agglomeration state of particles in suspension. Due to the amorphous shape and to sonication in dispersion medium, all four kinds of dental dust from composites Z250 and Z500

were found to agglomerate in larger units by weak physical interactions. From the DLS analysis, three main agglomerate peaks are visible. However, agglomerates are not fixed units and they can change their size and shape [33]. The geometric diameter measured in SEM and the hydrodynamic diameter measured using DLS will deviate as the methods are based on different principles. The size measured by DLS is usually greater than what is measured by other techniques [34], especially for realistic poly-dispersed and aggregated samples of various size ranges. DLS has been reported to yield more than 50% larger number-weighted medians than SEM – independent of size-range [35]. This can explain the differences seen when the DLS and SEM results are compared.

To determine if dental composites dust have possible toxic effects on the respiratory system, we have used a human bronchial epithelial cell line HBEC-3KT for our study to serve the purpose as an *in vitro* model to mimic the lung epithelium. Our model focused on the toxic cellular effects measured after three exposure time intervals of 24 h, 48 h and 72 h. These time intervals were chosen because dentists are occupationally exposed to dental composites particulates occurring on a daily basis during dental restoration procedures [15]. The exposure is primarily due to inhalation.

It has previously been demonstrated that inorganic filler particles of dental composites could induce an inflammatory response [29]. We have measured the toxicity effect of dental composites dust using LDH assay. To assess what the exposure levels are for dental health professionals and whether these levels can potentially lead to undesirable health effects we used a wide range between low and high doses. The same doses (5, 10, 20, 40 and 80 $\mu\text{g}/\text{cm}^2$) were used in Ansteinsson et al. [29]. Our results indicate that low doses do not show to have a toxicity effect on human bronchial epithelial cells. At the dose of 5 $\mu\text{g}/\text{cm}^2$, we observed negative values of mean % LDH released. Mathisen et al. demonstrated that low doses of filler particles and methacrylate monomer triethyleneglycol dimethacrylate (TEGDMA) can induce an additively attenuate effect in the inflammatory responses [36]. The negative effect may also suggest that cells could adapt metabolically to the dental composites at low doses possibly through a mechanism known as hormetic-like (biphasic) dose-response [37].

It has been demonstrated that surface chemistry and size of the particles have different ability to access the cell surface or become internalized within the intracellular space [38]. It could be possible that particles in longer times of exposure are modified or discharged by the cells in different ways [39,40].

All four of the dental composite dusts showed similar toxicity results when compared to the unexposed group. Higher concentrations (40 and 80 $\mu\text{g}/\text{cm}^2$) of the dental composites dusts are possibly provoking more cell membrane damage. In addition to that, dust from use of black diamond bur (which has a super-coarse grinding), creates more cell membrane damage and affecting the cell viability than use of the red diamond bur (typically used in dentist clinics for finishing dental composites) already after 24 h of exposure at lower concentrations. The length of the exposure time seems to play a role in increasing the cell toxicity in the higher concentrations tested. Regarding cell viability, after 72 h of exposure to low doses, we did not observe major changes in cell viability.

Electron micrographs of HBEC-3KT cells exposed at a concentration of 5 $\mu\text{g}/\text{cm}^2$ and 40 $\mu\text{g}/\text{cm}^2$ of Z500 black for 24 h and 72 h demonstrated that the human bronchial epithelial cells are taking up the dental dust of composites. Already after 24 h the dental dust composites are engulfed in membrane invaginations close to the nuclei. The particles are possibly engulfed through endocytosis mechanisms [41]. After 72 h of exposure, the composites particles appear to be observed inside smaller membrane vesicles as if they were processed or discharged by the cells. At the low dose of 5 $\mu\text{g}/\text{cm}^2$, the cells seem not to be affected or damaged by the engulfed particles. Future studies could focus on identifying the type of endocytic mechanisms and the pathway involved in the process. No dental composite particles are found inside the nuclei in any sample, even though these membrane invaginations are localized close to them.

5. Conclusion

The two types of dental resin composite materials grinded with fine and coarse burs generated ultrafine particles in number concentrations of $\sim 10^5 \text{ cm}^{-3}$. The results did not depend on the bur coarseness or on the type of resin composite and suggest that thermal decomposition of the matrix is a possible source of the ultrafine particles. However, additional investigations focusing on the source of the ultrafine particles is necessary. In addition, SEM investigations showed that more than 80% of the particles was smaller than 1 μm , which means dentists are exposed to a high fraction of respirable dusts. The grinding took place inside of a chamber, which is not comparable to exposure during real work procedures. Further research using personal samplers in dental clinics are needed for a thorough exposure assessment. Nevertheless, the data adds important information on size distributions and particle morphologies generated when working with different composite materials and burs.

Our results suggest that dental composites dusts can induce a toxicity response on human bronchial epithelial cells HBEC-3KT *in vitro*. The results showed that the toxic effect develops at high doses and after longer than 24 h time of exposure. Moreover dusts generate by a super course diamond bur appears to affect the integrity and cell viability more than dusts from a fine diamond bur. However, it is important to note that this work is based on a cellular *in vitro* study and that further *in vivo* and epidemiological research will be necessary to determine possible harmful health effects of dental composites.

Declaration of interests

The authors declare that they have no known competing financial interests or personal relationships that could have appeared to influence the work reported in this paper.

Acknowledgments

The project was financially supported by National Institute of Occupational Health and the Oral Health Centres of Exper-

tise in Eastern Norway (TKØ) in collaboration with the Nordic Institute of Dental Materials (NIOM, Oslo). Professor Mahmood Amiry-Moghaddam and laboratory engineer Mina Martine Frey from the Institute of Basic Medical Sciences at the University of Oslo are greatly acknowledged for use of their electron microscopy facilities as well as their expertise and excellent technical assistance. We also wish to thank Dr. Balazs Berlinger, formerly at NIOH, Dr. Raymond Olsen, STAMI, and Miss Anna Legfeldt for their valuable contributions in the initial phase of the project.

Appendix A. Supplementary data

Supplementary material related to this article can be found, in the online version, at doi:<https://doi.org/10.1016/j.dental.2021.03.011>.

REFERENCES

- [1] Zimmerli B, Strub M, Jeger F, Stadler O, Lussi A. Composite materials: composition, properties and clinical applications. A literature review. *Schweiz Monatsschr Zahnmed* 2010;120:972–86.
- [2] Ilie N, Hickel R. Resin composite restorative materials. *Aust Dent J* 2011;56(Suppl 1):59–66, <http://dx.doi.org/10.1111/j.1834-7819.2010.01296.x>.
- [3] Shin MA, Drummond JL. Evaluation of chemical and mechanical properties of dental composites. *J Biomed Mater Res* 1999;48:540–5, [http://dx.doi.org/10.1002/\(sici\)1097-4636\(1999\)48:4<540::aid-jbm21>3.3.co;2-v](http://dx.doi.org/10.1002/(sici)1097-4636(1999)48:4<540::aid-jbm21>3.3.co;2-v).
- [4] Beun S, Bogaerts P, Van Nieuwenhuysen JP. Manual or rotary root canal preparation? Nickel-titanium or stainless steel? Review of the literature. *Rev Belge Med Dent* (1984) 2005;60:81–91.
- [5] Pratap B, Gupta RK, Bhardwaj B, Nag M. Modeling based experimental investigation on polymerization shrinkage and micro-hardness of nano alumina filled resin based dental material. *J Mech Behav Biomed Mater* 2019;99:86–92, <http://dx.doi.org/10.1016/j.jmbbm.2019.06.026>.
- [6] Sabbagh J, Ryelandt L, Bacherius L, Biebuyck JJ, Vreven J, Lambrechts P, et al. Characterization of the inorganic fraction of resin composites. *J Oral Rehabil* 2004;31:1090–101, <http://dx.doi.org/10.1111/j.1365-2842.2004.01352.x>.
- [7] Soderholm KJ, Yang MC, Garcea I. Filler particle leachability of experimental dental composites. *Eur J Oral Sci* 2000;108:555–60, <http://dx.doi.org/10.1034/j.1600-0722.2000.00919.x>.
- [8] Van Landuyt KL, Hellack B, Van Meerbeek B, Peumans M, Hoet P, Wiemann M, et al. Nanoparticle release from dental composites. *Acta Biomater* 2014;10:365–74.
- [9] Van Landuyt KL, Yoshihara K, Geebelen B, Peumans M, Godderis L, Hoet P, et al. Should we be concerned about composite (nano-)dust? *Dent Mater* 2012;28:1162–70, <http://dx.doi.org/10.1016/j.dental.2012.08.011>.
- [10] Iliadi A, Koletsi D, Eliades T, Eliades G. Particulate production and composite dust during routine dental procedures. A systematic review with meta-analyses. *Materials* (Basel) 2020;13, <http://dx.doi.org/10.3390/ma13112513>.
- [11] Bogdan A, Buckett MI, Japuntich DA. Nano-sized aerosol classification, collection and analysis—method development using dental composite materials. *J Occup Environ Hyg* 2014;11:415–26, <http://dx.doi.org/10.1080/15459624.2013.875183>.
- [12] Bradna Pavel OL, Vladimir Zdimal, Tomas Navratil, Daniela Peclova. Detection of nanoparticles released at finishing of dental composite materials. *Monatsh Chem* 2017;531–7, <http://dx.doi.org/10.1007/s00706-016-1912-6>.
- [13] Sotiřiou M, Ferguson SF, Davey M, Wolfson JM, Demokritou P, Lawrence J, et al. Measurement of particle concentrations in a dental office. *Environ Monit Assess* 2008;137(1–3):351–61.
- [14] Godwin CC, Batterman SA, Sahni SP, Peng CY. Indoor environment quality in dental clinics: potential concerns from particulate matter. *Am J Dent* 2003;16:260–6.
- [15] Helmis CG, Tzoutzas J, Flocas HA, Halios CH, Stathopoulou OI, Assimakopoulos VD, et al. Indoor air quality in a dentistry clinic. *Sci Total Environ* 2007;377:349–65, <http://dx.doi.org/10.1016/j.scitotenv.2007.01.100>.
- [16] Commission EU, Council Directive 1999/30/EC of 22 April 1999 relating to limit values for sulphur dioxide, nitrogen dioxide and oxides of nitrogen, particulate matter and lead in ambient air, *Official Journal of the European Communities*. C. Information and notices 1999.
- [17] EPA USEPA. Latest findings on national air quality: 1997 status and trends. Office of Air Quality Planning and Standards Research Triangle Park; 1998.
- [18] Cokic SM, Asbach C, De Munck J, Van Meerbeek B, Hoet P, Seo JW, et al. The effect of water spray on the release of composite nano-dust. *Clin Oral Invest* 2020;24(7):2403–14.
- [19] Schmalz G, Hickel R, van Landuyt KL, Reichl FX. Nanoparticles in dentistry. *Dent Mater* 2017;33:1298–314, <http://dx.doi.org/10.1016/j.dental.2017.08.193>.
- [20] Borak J, Fields C, Andrews LS, Pemberton MA. Methyl methacrylate and respiratory sensitization: a critical review. *Crit Rev Toxicol* 2011;41:230–68, <http://dx.doi.org/10.3109/10408444.2010.532768>.
- [21] Jaakkola MS, Leino T, Tammilehto L, Ylostalo P, Kuosma E, Alanko K. Respiratory effects of exposure to methacrylates among dental assistants. *Allergy* 2007;62:648–54, <http://dx.doi.org/10.1111/j.1398-9995.2007.01379.x>.
- [22] Mikov I, Turkalj I, Jovanovic M. Occupational contact allergic dermatitis in dentistry. *Vojnosanit Pregl* 2011;68:523–5, <http://dx.doi.org/10.2298/vsp1106523m>.
- [23] Rubel DM, Watchorn RB. Allergic contact dermatitis in dentistry. *Australas J Dermatol* 2000;41:63–9, <http://dx.doi.org/10.1046/j.1440-0960.2000.00398.x>.
- [24] Kahraman H, Koksall N, Cinkara M, Ozkan F, Sucakli MH, Ekerbicer H. Pneumoconiosis in dental technicians: HRCT and pulmonary function findings. *Occup Med (Lond)* 2014;64:442–7, <http://dx.doi.org/10.1093/occmed/kqu047>.
- [25] Leggat PA, Kedjarune U, Smith DR. Occupational health problems in modern dentistry: a review. *Ind Health* 2007;45:611–21, <http://dx.doi.org/10.2486/indhealth.45.611>.
- [26] Oberdorster G, Elder A, Rinderknecht A. Nanoparticles and the brain: cause for concern? *J Nanosci Nanotechnol* 2009;9:4996–5007, <http://dx.doi.org/10.1166/jnn.2009.gr02>.
- [27] Eide J, Gylseth B, Skaug V. Silicotic lesions of the bone marrow: histopathology and microanalysis. *Histopathology* 1984;8:693–703, <http://dx.doi.org/10.1111/j.1365-2559.1984.tb02381.x>.
- [28] Slavin RE, Swedo JL, Brandes D, Gonzalez-Vitale JC, Osornio-Vargas A. Extrapulmonary silicosis: a clinical, morphologic, and ultrastructural study. *Hum Pathol* 1985;16:393–412, [http://dx.doi.org/10.1016/s0046-8177\(85\)80233-1](http://dx.doi.org/10.1016/s0046-8177(85)80233-1).
- [29] Ansteinsson VE, Samuelsen JT, Dahl JE. Filler particles used in dental biomaterials induce production and release of inflammatory mediators in vitro. *J Biomed Mater Res B Appl Biomater* 2009;89:86–92, <http://dx.doi.org/10.1002/jbm.b.31190>.
- [30] Jensen K, Kembouche Y, Christiansen E, Jacobsen N, Wallin H, Guiot C. The Generic NANOGENOTOX Dispersion

- Protocol: Final Protocol for Producing Suitable Manufactured Nanomaterial Exposure Media. NANOGENOTOX Joint Action, European Commission; 2011. Available online: www.nanogenotox.eu/files/PDF/web%20nanogenotox%20dispersion%20protocol.pdf.
- [31] Lebedova J, Hedberg YS, Odnevall Wallinder I, Karlsson HL. Size-dependent genotoxicity of silver, gold and platinum nanoparticles studied using the mini-gel comet assay and micronucleus scoring with flow cytometry. *Mutagenesis* 2018;33:77–85, <http://dx.doi.org/10.1093/mutage/gex027>.
- [32] Phuyal S, Kasem M, Rubio L, Karlsson HL, Marcos R, Skaug V, et al. Effects on human bronchial epithelial cells following low-dose chronic exposure to nanomaterials: a 6-month transformation study. *Toxicol In Vitro* 2017;44:230–40, <http://dx.doi.org/10.1016/j.tiv.2017.07.016>.
- [33] Walter D. In: D.F. (DFG)s, editor. *Primary particles – agglomerates – aggregates*. Nanomaterials: Bonn, Germany; 2013.
- [34] Dhawan A, Sharma V. Toxicity assessment of nanomaterials: methods and challenges. *Anal Bioanal Chem* 2010;398:589–605, <http://dx.doi.org/10.1007/s00216-010-3996-x>.
- [35] Babick F, Mielke J, Wohlleben W, Weigel S, Hodoroaba VD. How reliably can a material be classified as a nanomaterial? Available particle-sizing techniques at work. *J Nanopart Res* 2016;18:158, <http://dx.doi.org/10.1007/s11051-016-3461-7>.
- [36] Mathisen GH, Ansteinsson V, Samuelsen JT, Becher R, Dahl JE, Bolling AK. TEGDMA and filler particles from dental composites additively attenuate LPS-induced cytokine release from the macrophage cell line RAW 264.7. *Clin Oral Investig* 2015;19:61–9, <http://dx.doi.org/10.1007/s00784-014-1212-7>.
- [37] Calabrese EJ. Biphasic dose responses in biology, toxicology and medicine: accounting for their generalizability and quantitative features. *Environ Pollut* 2013;182:452–60, <http://dx.doi.org/10.1016/j.envpol.2013.07.046>.
- [38] Murdock RC, Braydich-Stolle L, Schrand AM, Schlager JJ, Hussain SM. Characterization of nanomaterial dispersion in solution prior to in vitro exposure using dynamic light scattering technique. *Toxicol Sci* 2008;101:239–53, <http://dx.doi.org/10.1093/toxsci/kfm240>.
- [39] Albrecht C, Hohr D, Haberzettl P, Becker A, Borm PJ, Schins RP. Surface-dependent quartz uptake by macrophages: potential role in pulmonary inflammation and lung clearance. *Inhal Toxicol* 2007;19(Suppl 1):39–48, <http://dx.doi.org/10.1080/08958370701492979>.
- [40] Albrecht C, Knaapen AM, Becker A, Hohr D, Haberzettl P, van Schooten FJ, et al. The crucial role of particle surface reactivity in respirable quartz-induced reactive oxygen/nitrogen species formation and APE/Ref-1 induction in rat lung. *Respir Res* 2005;6:129, <http://dx.doi.org/10.1186/1465-9921-6-129>.
- [41] Behzadi S, Serpooshan V, Tao W, Hamaly MA, Alkawareek MY, Dreaden EC, et al. Cellular uptake of nanoparticles: journey inside the cell. *Chem Soc Rev* 2017;46:4218–44, <http://dx.doi.org/10.1039/c6cs00636a>.

Update

Dental Materials

Volume 38, Issue 9, September 2022, Page 1564

DOI: <https://doi.org/10.1016/j.dental.2022.07.007>



Available online at www.sciencedirect.com

ScienceDirect

journal homepage: www.elsevier.com/locate/dental



Corrigendum

Corrigendum to “Characterization and toxicity evaluation of air-borne particles released by grinding from two dental resin composites in vitro” [Dent Mater 37 (7) (2021) 1121–33]



L.M.A. Camassa^a, T.K. Ervik^a, F.D. Zegeye^a, I. Mdala^b, H. Valen^{c,d}, V. Ansteinsson^a, Shan Zienolddiny-Narui^{a,*}

^a National Institute of Occupational Health, Oslo, Norway

^b Institute of Health and Society, University of Oslo, Oslo, Norway

^c Nordic Institute of Dental Materials, Oslo, Norway

^d Oral Health Centres of Expertise in Eastern Norway, Oslo, Norway

The authors would like to inform the readers of a needed clarification in this article regarding a missing acknowledgement:

Acknowledgements

This project was cofunded by NIOH and the Research Council of Norway, under NanoBioReal project ID No. 288768 "towards a reliable assessment of nanomaterial health effects using advanced biological models and assays" by the Nano2021 research program.

DOI of original article: <https://doi.org/10.1016/j.dental.2021.03.011>

* Corresponding author.

E-mail address: shan.narui@stami.no (S. Zienolddiny-Narui).

<https://doi.org/10.1016/j.dental.2022.07.007>

0109-5641/© 2022 Published by Elsevier Inc. on behalf of The Academy of Dental Materials.